Proc. Natl. Acad. Sci. USA
Vol. 92, pp. 10227–10231, October 1995
Neurobiology

Vector-mediated delivery of ^{125}I-labeled β-amyloid peptide Aβ$^{1-40}$ through the blood–brain barrier and binding to Alzheimer disease amyloid of the Aβ$^{1-40}$/vector complex

(monoclonal antibody/drug delivery/streptavidin/biotin)

YASUNARI SAITO, JODY BUCIAK, JING YANG, AND WILLIAM M. PARDRIDGE*

Department of Medicine, School of Medicine, University of California, Los Angeles, CA 90024

Communicated by Charles H. Sawyer, University of California School of Medicine, Los Angeles, CA, July 10, 1995 (received for review May 24, 1995)

ABSTRACT **The brain amyloid of Alzheimer disease (AD) may potentially be imaged in patients with AD by using neuroimaging technology and a radiolabeled form of the 40-residue β-amyloid peptide Aβ$^{1-40}$ that is enabled to undergo transport through the brain capillary endothelial wall, which makes up the blood–brain barrier (BBB) *in vivo*. Transport of ^{125}I-labeled Aβ$^{1-40}$ (^{125}I-Aβ$^{1-40}$) through the BBB was found to be negligible by experiments with both an intravenous injection technique and an internal carotid artery perfusion method in anesthetized rats. In addition, ^{125}I-Aβ$^{1-40}$ was rapidly metabolized after either intravenous injection or internal carotid artery perfusion. BBB transport was increased and peripheral metabolism was decreased by conjugation of monobiotinylated ^{125}I-Aβ$^{1-40}$ to a vector-mediated drug delivery system, which consisted of a conjugate of streptavidin (SA) and the OX26 monoclonal antibody to the rat transferrin receptor, which undergoes receptor-mediated transcytosis through the BBB. The brain uptake, expressed as percent of injected dose delivered per gram of brain, of the ^{125}I,bio-Aβ$^{1-40}$/SA-OX26 conjugate was 0.15 ± 0.01, a level that is 2-fold greater than the brain uptake of morphine. The binding of the ^{125}I,bio-Aβ$^{1-40}$/SA-OX26 conjugate to the amyloid of AD brain was demonstrated by both film and emulsion autoradiography performed on frozen sections of AD brain. Binding of the ^{125}I,bio-Aβ$^{1-40}$/SA-OX26 conjugate to the amyloid of AD brain was completely inhibited by high concentrations of unlabeled Aβ$^{1-40}$. In conclusion, these studies show that BBB transport and access to amyloid within brain may be achieved by conjugation of Aβ$^{1-40}$ to a vector-mediated BBB drug delivery system.**

Alzheimer disease (AD) is a severe neurodegenerative disorder, and presently there is no premortem diagnostic test for this disease (1). The dementia of AD correlates with the deposition in brain of amyloid (2), which is principally composed of the 42- to 43-amino acid β-amyloid peptide, Aβ$^{1-42/43}$ (3, 4). One possible diagnostic approach to AD is the development of a premortem brain scan that would allow for semiquantitation of the Aβ amyloid burden in human brain. Previous studies have shown that ^{125}I-labeled Aβ$^{1-40}$ (^{125}I-Aβ$^{1-40}$) binds to preexisting amyloid plaques in frozen sections of AD brain (5). The delivery to brain of radiolabeled Aβ$^{1-40}$ in conjunction with the use of standard neuroimaging modalities such as single photon emission computed tomography (SPECT) may allow for quantitation of Aβ amyloid in AD brain. Therefore, the present studies examine whether ^{125}I-Aβ$^{1-40}$ undergoes significant transport through the brain capillary endothelial wall, which makes up the blood–brain barrier (BBB) *in vivo*, by using both intravenous/pharmacokinetic and internal carotid artery perfusion techniques. These studies then measure the extent to which BBB transport of ^{125}I-Aβ$^{1-40}$ is enhanced with the use of a vector-mediated drug delivery system (6). The latter is composed of a conjugate of streptavidin (SA) and the OX26 monoclonal antibody (mAb) to the transferrin receptor (7), which undergoes receptor-mediated transcytosis through the BBB (6); ^{125}I-Aβ$^{1-40}$ is monobiotinylated (bio), and ^{125}I,bio-Aβ$^{1-40}$ is then conjugated to the SA-OX26 vector. Since conjugation of ^{125}I-Aβ$^{1-40}$ to the vector-mediated delivery system may inhibit binding of Aβ$^{1-40}$ to amyloid plaques, the present studies also examine the saturable binding of ^{125}I-Aβ$^{1-40}$ to amyloid in AD brain after conjugation to the delivery system.

MATERIALS AND METHODS

Materials. Male Sprague–Dawley rats (weighing 200–270 g) were obtained from Harland–Sprague–Dawley. Human Aβ$^{1-40}$ was purchased from Bachem. [^{125}I]Iodine was obtained from Amersham. Sulfosuccinimidyl 2-(biotinamido)ethyl-1,3′-dithiopropionate (NHS-SS-biotin) was obtained from Pierce. Biotin-XX-NHS was supplied by Calbiochem, where XX = bis(aminohexanoyl) spacer arm and NHS = *N*-hydroxysuccinimide. Recombinant SA and all other reagents were obtained from Sigma.

Aβ$^{1-40}$ Iodination. Aβ$^{1-40}$ (10 μg, 2.4 nmol) was iodinated with [^{125}I]iodine [2 mCi (1 mCi = 37 MBq), 1.0 nmol] and chloramine T (39 nmol) to a specific activity of 40.8 μCi//μg and a trichloroacetic acid (TCA) precipitability of 99.1%. The ^{125}I-Aβ$^{1-40}$ eluted from a C_4 reverse-phase HPLC column as a single peak at 37% acetonitrile. The elution of a single iodinated species is consistent with the presence of a single tyrosine in Aβ$^{1-40}$, at residue 10 (4).

Conjugate Synthesis. The OX26 was conjugated to SA by a thioether linkage as described previously (7, 8). The brain delivery of [^{3}H]biotin bound to the SA-OX26 conjugate after intravenous injection was measured as described previously (9). Uptake of the [^{3}H]biotin/SA-OX26 conjugate at 60 min after intravenous injection was 0.21 ± 0.03 percent of the injected dose (%ID) per gram of brain, with a BBB permeability–surface area (PS) product of 1.68 ± 0.31 μl/min per g, a 60-min plasma area under the plasma concentration curve (AUC) of 129 ± 18 %ID·min/ml, and a brain volume of distribution (V_D) of 168 ± 29 μl/g.

The publication costs of this article were defrayed in part by page charge payment. This article must therefore be hereby marked "*advertisement*" in accordance with 18 U.S.C. §1734 solely to indicate this fact.

Abbreviations: Aβ$^{1-40}$, β-amyloid peptide residues 1–40; BBB, blood–brain barrier; AD, Alzheimer disease; SA, streptavidin; mAb, monoclonal antibody; OX26, murine mAb to the rat transferrin receptor; NHS, *N*-hydroxysuccinimide; SPECT, single photon emission computed tomography; bio, biotinylated; V_D, brain volume of distribution; PS, permeability–surface area; AUC, area under the plasma concentration curve; TCA, trichloroacetic acid; TFA, trifluoroacetic acid; %ID, percent of the injected dose.

*To whom reprint requests should be addressed.

Biotinylation of ^{125}I-Aβ^{1-40}. ^{125}I-Aβ^{1-40} was monobiotinylated with either NHS-XX-biotin or NHS-SS-biotin to generate ^{125}I,bio-XX-Aβ^{1-40} or ^{125}I,bio-SS-Aβ^{1-40}, as described previously for neuropeptides (8). The XX linker inserts a noncleavable (amide) 14-atom spacer between the Aβ^{1-40} and the biotin (10). The SS linker inserts a cleavable (disulfide) 8-atom spacer between the Aβ^{1-40} and the biotin (Fig. 1). The ^{125}I,bio-Aβ^{1-40} conjugated to SA-OX26 was purified by Toyo Soda Kasei (TSK) gel filtration HPLC with an isocratic elution at 0.5 ml/min in 0.1 M Na_2HPO_4/0.5 M NaCl, pH 7.0/0.05% Tween-20. The conjugate peak was collected at an elution volume of 7–9 ml, which was well separated from the unconjugated ^{125}I-Aβ^{1-40}, which eluted at 13-14 ml. A low molar ratio (4:1) of either NHS-SS-biotin or NHS-XX-biotin to Aβ^{1-40} was used to ensure monobiotinylation of the Aβ peptide. Owing to the multivalency of the binding of biotinylated substrate by the SA-OX26 conjugate, monobiotinylation of ligands must be performed to prevent the formation of high molecular weight aggregates (7). Electrospray mass spectrometry was performed on unlabeled biotinylated Aβ^{1-40} (designated bio-Aβ^{1-40}) at the mass spectrometry core facility at the Beckman Research Institute at the City of Hope Hospital (Duarte, CA). The mass of the bio-Aβ^{1-40} was 4784 Da, while the predicted mass of monobiotinylated Aβ^{1-40} is 4783. The exact site of biotinylation is not known but is presumed to be Lys-16 or Lys-28 of Aβ^{1-40}, since the succinimide esters biotinylate free amino groups (10). The complex of ^{125}I,bio-Aβ^{1-40} and the SA-OX26 conjugate is designated ^{125}I,bio-Aβ^{1-40}/SA-OX26 (Fig. 1).

The ^{125}I-Aβ^{1-40} monobiotinylated with NHS-XX-biotin is designated ^{125}I,bio-XX-Aβ^{1-40}. The ^{125}I-Aβ^{1-40} peptide monobio tinylated with NHS-SS-biotin is designated ^{125}I,bio-SS-Aβ^{1-40}. To demonstrate cleavage of the disulfide linker, the ^{125}I,bio-SS-Aβ^{1-40} was bound to the SA-OX26 conjugate, and the complex was treated with dithiothreitol (0.05 M, pH 7.0) for 30 min at room temperature prior to injection onto the TSK gel filtration HPLC column (G2000 SW_{XL}, TosoHaas, Montgomeryville, PA).

Intravenous Injection Technique. The pharmacokinetics and brain delivery of ^{125}I-Aβ^{1-40}, either alone or conjugated to the SA-OX26 vector, were determined after a single intravenous injection in anesthetized rats, as described previously (9). Pharmacokinetic parameters were determined by fitting plasma TCA-precipitable radioactivity data to either a mono- or bi-exponential equation (12), as described previously (9). The V_D of the ^{125}I-Aβ was determined from the dpm/g of brain divided by dpm/μl of corresponding terminal plasma at 0.5 or 2.0 hr after injection. The BBB PS product of the ^{125}I,bio-Aβ^{1-40}/SA-OX26 was calculated from V_D, the brain plasma volume (10 μl/g), and the $AUC|^t_0$, as described previously (9). The brain delivery of ^{125}I-Aβ^{1-40}, either alone or conjugated to the SA-OX26 vector, was expressed as %ID per gram of brain and was computed from the PS and $AUC|^t_0$ as described previously (9).

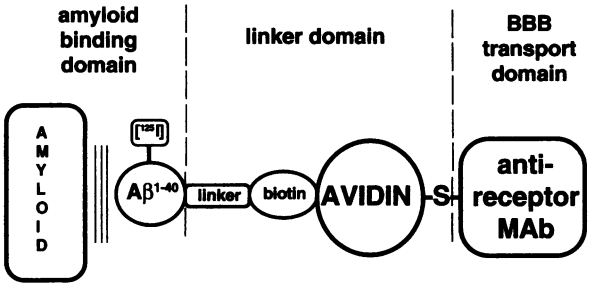

FIG. 1. Delivery of ^{125}I-Aβ^{1-40} through the BBB and binding to brain amyloid of AD. The delivery system comprises three domains: an amyloid binding domain consisting of the radiolabeled Aβ^{1-40}; a linker domain, consisting of an 8- to 14-atom linker joining the Aβ^{1-40} and the biotin moiety, which is in turn bound to an avidin analogue; and a BBB transport domain, which consists of an anti-receptor mAb joined to the avidin analogue through a stable thioether (-S-) bond. The avidin analogue may consist of avidin (6), SA, as used in the present study, or neutral avidin (NLA), as used in previous studies (9). The BBB transport domain may consist of an mAb, such as the OX26 antibody to the transferrin receptor for studies in rats, or the 83-14 antibody to the insulin receptor for applications in either humans or Old World primates (11). If the linker is formed with NHS-SS-biotin, then an 8-atom disulfide (cleavable) linker is inserted between the Aβ^{1-40} and the biotin moiety, and consists of —$(CH_2)_2$—S—S—$(CH_2)_2$NHCO—. If a noncleavable (amide) linkage is placed between the Aβ^{1-40} and the biotin moiety, such as with NHS-XX-biotin, then a 14-atom spacer is present consisting of —$(CH_2)_5$NHCO$(CH_2)_5$NHCO)— (10).

Internal Carotid Artery Perfusion Technique. The transport of ^{125}I-Aβ^{1-40} through the BBB was measured in ketamine-anesthetized rats by using the internal carotid artery perfusion/capillary depletion technique described previously (13). The purpose of the capillary depletion step is to differentiate peptide adsorption to the vasculature (which causes the peptide homogenate V_D to exceed the sucrose V_D), from actual peptide transport into brain (13). BBB transport may be indicated when the postvascular supernatant V_D for the peptide exceeds that for sucrose. However, the postvascular supernatant must be corrected for metabolism by multiplying the postvascular supernatant V_D by the fractional TCA-precipitable homogenate ^{125}I radioactivity (13).

Autoradiography and Immunocytochemistry. The ability of the ^{125}I,bio-XX-Aβ^{1-40} to bind to the amyloid of AD despite conjugation to the SA-OX26 vector was examined with both film and emulsion autoradiography (5). The noncleavable amide linker was used to prevent cleavage of the ^{125}I,bio-Aβ^{1-40} from the SA-OX26 by tissue disulfide reductases. Snap-frozen AD cortex was provided by the University of California at Los Angeles Department of Pathology/Neuropathology, and 15-μm sections were cut on a cryostat and thaw-mounted to gelatin-coated slides. To each slide was added 250 μl of TBM buffer (TBM = 0.05 M Tris·HCl, pH 7.4/10 mM $MnCl_2$/0.1% bovine serum albumin) containing ^{125}I,bio-XX-Aβ^{1-40}/SA-OX26 at 0.5 μCi/ml and 0 or 10 μM unlabeled Aβ^{1-40}. The slides were incubated at room temperature for 2 hr, washed, and air-dried at 4°C. For film autoradiography, the fully dried slides were placed in opposition to Kodak X-Omat AR x-ray film and exposed for 1 week at −20°C. Other slides were used for emulsion autoradiography followed by either darkfield or brightfield photography.

Frozen sections of AD brain were also fixed in 10% Formalin (10 min, 4°C), treated with 50% formic acid for 15 min at 23°C, and immunostained with a thyroglobulin-absorbed rabbit polyclonal antiserum (1:1000 dilution) prepared against a conjugate of Aβ^{1-28} and bovine thyroglobulin, as described previously (14), and lightly counterstained with Mayer's hematoxylin. The immunocytochemistry and emulsion autoradiography slides were photographed and were scanned with a Nikon Coolscan external slide scanner.

RESULTS

Intravenous Injection of Unconjugated ^{125}I-Aβ^{1-40}. The pharmacokinetics and brain uptake of intravenously injected ^{125}I-Aβ^{1-40} were evaluated for the first 30 min after intravenous injection (Fig. 2). More than 95% of the injected dose was removed from blood by 30 min after administration (Fig. 2). The ^{125}I-Aβ^{1-40} was also rapidly metabolized after intravenous administration, and the TCA precipitability of the plasma radioactivity fell from 92.7% ± 1.5% at 0.25 min after injection to 41.3% ± 3.5% at 30 min after injection (Fig. 2). The pharmacokinetic parameters for unconjugated ^{125}I-Aβ^{1-40} are given in Table 1. The plasma clearance, 10.1 ± 1.2 ml/min·kg, is equal to the previously reported plasma clearance for [^{14}C]sucrose, 10.8 ± 0.4 ml/min·kg (15), suggesting that the

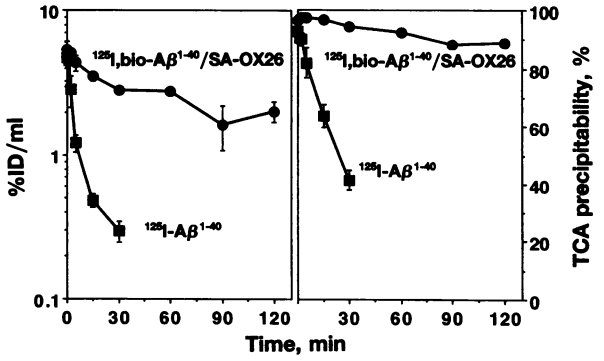

FIG. 2. (*Left*) %ID/ml of plasma is plotted versus the time after intravenous injection of either ^{125}I,bio-Aβ$^{1-40}$/SA-OX26 or unconjugated ^{125}I-Aβ$^{1-40}$. (*Right*) Serum TCA precipitability is shown. Results are mean ± SEM (n = 3 rats per point).

principal route of removal of ^{125}I-Aβ$^{1-40}$ from the circulation is glomerular filtration. The brain uptake of ^{125}I-Aβ$^{1-40}$ after intravenous administration was low, 0.0089 ± 0.0008 %ID/g of brain (Fig. 3). The TCA precipitability of the brain homogenate radioactivity 30 min after injection was low at 35% ± 3% (mean ± SEM, n = 3 rats), consistent with the rapid metabolism of circulating ^{125}I-Aβ$^{1-40}$ (Fig. 2). Owing to the rapid metabolism of peripherally administered ^{125}I-Aβ$^{1-40}$, it was not possible to compute the BBB PS product for the unconjugated ^{125}I-Aβ$^{1-40}$, but the low brain uptake (Fig. 3) indicated negligible BBB permeability to the unconjugated Aβ$^{1-40}$ peptide.

Internal Carotid Artery Perfusion of Unconjugated ^{125}I-Aβ$^{1-40}$. To evaluate BBB transport of ^{125}I-Aβ$^{1-40}$ in the absence of peripheral metabolism of peptide, internal carotid artery perfusions were performed. The 5-min V_D of ^{125}I-Aβ$^{1-40}$ is 17.3 ± 7.8 μl/g and the vascular pellet V_D was 0.79 ± 0.50 μl/g (Table 2). However, the ^{125}I-Aβ$^{1-40}$ peptide was rapidly metabolized by brain after internal carotid artery perfusion, and the homogenate TCA precipitability after the 5-min perfusion was 51% ± 19% (Table 2). Therefore, the TCA-precipitable volume of distribution of Aβ$^{1-40}$ in the postvascular supernatant (determined by multiplying the supernatant V_D by the fractional TCA precipitation) is 8.0 ± 5.1 μl/g.

Pharmacokinetics and Brain Delivery of ^{125}I-Aβ$^{1-40}$ Conjugated to the SA-OX26 Vector. The ^{125}I,bio-SS-Aβ$^{1-40}$/SA-OX26 conjugate migrated through the TSK gel filtration HPLC column (Fig. 4) in a 7- to 9-ml elution volume, which is identical to the elution volume of [^{3}H]biotin/SA-OX26. When the conjugate was treated with 50 mM dithiothreitol at pH 7.0 for 30 min prior to injection onto the TSK column, the majority of the radioactivity shifted to the salt volume of the column, consistent with elution of the desbiotinylated ^{125}I-Aβ$^{1-40}$ after cleavage from the SA-OX26 vector (Fig. 4).

Table 1. Pharmacokinetic parameters

Parameter	^{125}I-Aβ$^{1-40}$	^{125}I,bio-Aβ$^{1-40}$/SA-OX26
k_1, min^{-1}	0.39 ± 0.10	0.012 ± 0.004
k_2, min^{-1}	0.027 ± 0.004	—
A_1, %ID/ml	4.9 ± 1.3	4.6 ± 0.3
A_2, %ID/ml	0.68 ± 0.16	—
$t^1_{1/2}$, min	2.0 ± 0.6	71 ± 25
$t^2_{1/2}$, min	27 ± 4	—
AUC$\|^{\infty}_0$, %ID·min/ml	38 ± 4	467 ± 139
V_{SS}, ml/kg	273 ± 59	106 ± 5
CL, ml/min·kg	10.1 ± 1.2	1.2 ± 0.4
MRT, min	27 ± 4	103 ± 37

Values were determined from data in Fig. 2 for 30 min and 120 min for ^{125}I-Aβ$^{1-40}$ and ^{125}I,bio-Aβ$^{1-40}$/SA-OX26, respectively. Best fits were obtained in the nonlinear regression analysis by fitting the ^{125}I-Aβ$^{1-40}$ data in Fig. 1 to a bi-exponential function and the ^{125}I,bio-Aβ$^{1-40}$/SA-OX26 data in Fig. 1 to a mono-exponential function (12). Dose per rat = 4.5 μCi of ^{125}I,bio-Aβ$^{1-40}$ conjugated to 30 μg of SA-OX26. k_1 and k_2, first and second components of rate constants for clearance; A, plasma concentration; V_{SS}, steady-state whole body volume of distribution; CL, clearance from plasma; MRT, mean residence time in plasma.

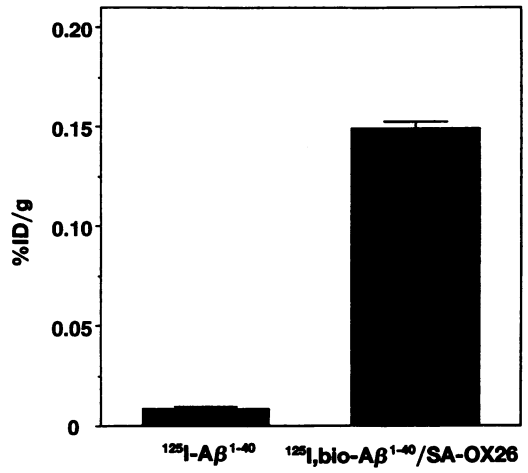

FIG. 3. %ID delivered per gram of brain for either ^{125}I-Aβ$^{1-40}$ at 30 min after injection or ^{125}I,bio-Aβ$^{1-40}$/SA-OX26 at 2 hr after injection. Results are mean ± SEM (n = 3).

The rate of metabolism and plasma clearance of ^{125}I,bio-Aβ$^{1-40}$ conjugated to the SA-OX26 vector was retarded compared with the metabolism and plasma clearance of the unconjugated ^{125}I-Aβ$^{1-40}$ peptide (Fig. 2). The metabolic stability of the conjugated peptide is demonstrated by the high level of TCA precipitability at 2 hr after injection: 89% ± 2% and 93% ± 1% in the plasma and brain homogenate compartments, respectively (mean ± SEM, n = 3 rats). The plasma clearance of the ^{125}I-Aβ$^{1-40}$ peptide was reduced nearly 90% after conjugation to the SA-OX26 vector (Table 1).

V_D at 120 min after injection of the ^{125}I,bio-Aβ$^{1-40}$/SA-OX26 conjugate was 86 ± 13 μl/g, the 2-hr AUC was 309 ± 43 %ID·min/ml, and the BBB PS product was 0.50 ± 0.09 μl/min·g. The brain delivery of the conjugate was 0.149 ± 0.004 %ID/g (Fig. 3), a level of brain uptake that is 2-fold greater than the maximal brain uptake of morphine, a neuroactive small molecule (16).

Autoradiography. ^{125}I,bio-Aβ$^{1-40}$/SA-OX26 bound to the amyloid in frozen sections of AD brain. As shown in Fig. 5*B*, the silver grains in the emulsion autoradiography collected over structures with a size identical to that of immunoreactive Aβ amyloid plaques detected with immunocytochemistry (Fig. 5*A*). The binding of the ^{125}I,bio-Aβ$^{1-40}$/SA-OX26 conjugate to the amyloid plaques was saturable, as inclusion of 10 μM unlabeled Aβ$^{1-40}$ completely prevented binding of the conjugate to the amyloid plaques as shown by film autoradiography (Fig. 5 *C* and *D*). This saturability of the binding of the

Table 2. V_D of ^{125}I-Aβ$^{1-40}$ after a 5-min internal carotid artery perfusion

Tracer	Brain fraction	V_D, μl/g
^{125}I-Aβ$^{1-40}$	Homogenate	17.3 ± 7.8
	Postvascular supernatant	8.0 ± 5.1
	Vascular pellet	0.79 ± 0.50
[^{14}C]Sucrose	Postvascular supernatant	8.0 ± 0.3

Results are mean ± SEM (n = 5) for a 5-min perfusion. The supernatant V_D for ^{125}I-Aβ$^{1-40}$ is the product of (measured supernatant V_D) × (brain TCA-precipitable radioactivity). The homogenate TCA-precipitable radioactivity fraction is 51% ± 19% (mean ± SEM, n = 5). The [^{14}C]sucrose data are from ref. 13. Perfusate contained ^{125}I-Aβ$^{1-40}$ at 3 μCi/ml.

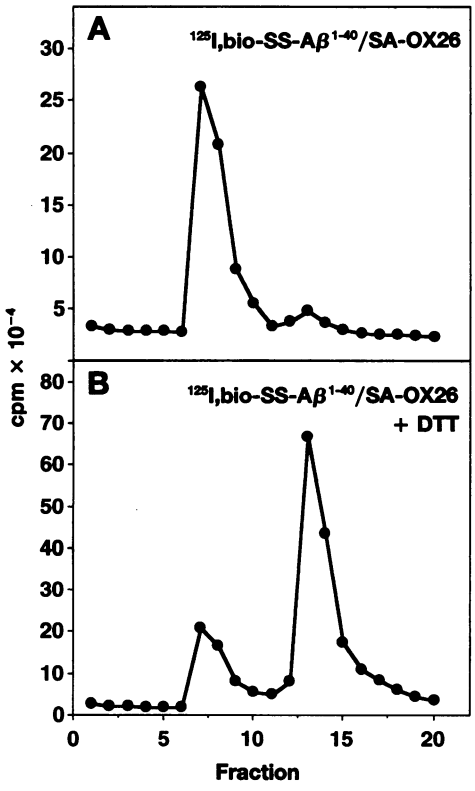

FIG. 4. Gel filtration HPLC of ^{125}I,bio-SS-Aβ$^{1-40}$ conjugated to the SA-OX26 vector before (*A*) or after (*B*) treatment with 50 mM dithiothreitol (DTT) for 30 min at pH 7.0 prior to injection into the column. Fraction size = 1.0 ml.

^{125}I,bio-Aβ$^{1-40}$/SA-OX26 conjugate to the amyloid plaques was also demonstrated by emulsion autoradiography.

DISCUSSION

The results of these studies are consistent with the following conclusions. First, unconjugated Aβ$^{1-40}$ undergoes negligible transport through the BBB *in vivo* but is rapidly degraded after either systemic administration or internal carotid artery perfusion (Fig. 2, Table 2). Second, conjugation of ^{125}I,bio-Aβ$^{1-40}$ to the SA-OX26 vector results in marked increase in brain uptake of Aβ$^{1-40}$ (Fig. 3), and this is due to the combined effects of increased BBB PS product (*Results*) and increased plasma AUC (Table 1). Third, the vector-conjugated form of Aβ$^{1-40}$ still avidly binds to amyloid plaques of AD by a saturable process (Fig. 5).

After intravenous administration, the brain uptake of unconjugated Aβ$^{1-40}$ is minimal (Fig. 3), and this is confirmed by studies with internal carotid artery perfusion (Table 2). The brain homogenate V_D for ^{125}I-Aβ$^{1-40}$ is approximately 2-fold greater than the homogenate V_D for a plasma volume marker, such as [^{14}C]sucrose (Table 2). Since sucrose does not undergo measurable transport through the BBB during a 5-min perfusion, the elevated V_D has been interpreted as evidence for BBB transport of ^{125}I-Aβ$^{1-40}$ (17). However, when the supernatant V_D is corrected for metabolism by using the fractional TCA precipitation (13), the corrected postvascular supernatant V_D for ^{125}I-Aβ$^{1-40}$ is not significantly different from the postvascular supernatant V_D for sucrose (Table 2), indicating lack of measurable transport of the intact peptide through the BBB *in vivo*. These results suggest that ^{125}I-Aβ$^{1-40}$ is adsorbed in the brain microvasculature and metabolized without significant transport into brain (Table 2). These conclusions are corroborated by other studies showing that Aβ$^{1-40}$ is rapidly adsorbed to surfaces and metabolized (18) and undergoes negligible transport through epithelial cell membranes (19). The rapid metabolism of Aβ$^{1-40}$ is due to the susceptibility of this peptide to a variety of proteases (20). However, this proteolysis is substantially reduced subsequent to aggregation of the Aβ$^{1-40}$ into amyloidotic fibrils (20).

Conjugation of ^{125}I,bio-Aβ$^{1-40}$ to the SA-OX26 vector results in a marked increase in brain delivery of the peptide (Fig. 3). The brain uptake of a peptide (expressed as %ID/g of brain) is a dual function of both the BBB PS product and the plasma AUC (*Materials and Methods*), and the vector-mediated brain uptake of the peptide is due to an increase in both the BBB PS product (*Results*) and the plasma AUC (Table 1). Conjugation of the Aβ$^{1-40}$ peptide to the SA-OX26 vector also inhibits the peripheral metabolism of the peptide (Fig. 2 *Right*). The brain uptake of the conjugated Aβ$^{1-40}$ peptide, 0.15 %ID/g (Fig. 3), is approximately 2-fold greater than the maximal brain uptake of morphine, a neuroactive small molecule (16).

The enhanced brain uptake and decreased metabolism of Aβ$^{1-40}$ after conjugation to the vector-mediated delivery system provides a setting wherein radiolabeled Aβ$^{1-40}$ peptide may then bind to preexisting amyloid plaques. However, conjugation of the Aβ$^{1-40}$ peptide to the delivery system must not impair Aβ$^{1-40}$ binding to amyloid. The Aβ is monobiotinylated at either Lys-16 or Lys-28 (*Materials and Methods*), and it is conceivable that biotinylation to these lysine residues may impair Aβ$^{1-40}$ binding to amyloid plaques. However, the XX-biotin linker used in these studies provides a 14-atom spacer between the ε-amino group of the peptide lysine and the actual biotin moiety which is bound to the SA-OX26 conjugate (Fig. 1). This long spacer arm has the potential to minimize steric hindrance, and the film and emulsion autoradiography studies show avid binding of the ^{125}I-Aβ$^{1-40}$ peptide to preexisting amyloid despite conjugation of ^{125}I-Aβ$^{1-40}$ to the SA-OX26 vector (Fig. 5). This binding is saturable by unlabeled Aβ$^{1-40}$ (Fig. 5). The size of the plaques seen with film autoradiography (Fig. 5*C*) is much greater than the size of the plaque visible in either emulsion radiography (Fig. 5*B*) or immunocytochemistry (Fig. 5*A*), suggesting that multiple small contiguous plaques may coalesce to give an amplified autoradiograph signal seen in film autoradiography.

Once transported across the BBB, Aβ$^{1-40}$ may bind to the extracellular amyloid found in either neuritic plaques or amyloid surrounding intracortical microvessels (21, 22). The access of Aβ$^{1-40}$ to this amyloid in AD via uptake of unconjugated Aβ$^{1-40}$ at the pial surface of the brain (23) is limited, because the pial route is a quantitatively insignificant component of peptide drug delivery to the brain (6). Unconjugated Aβ$^{1-40}$ does not undergo significant transport through the BBB (Table 2), and the BBB is intact in AD (24). Therefore, the delivery of Aβ$^{1-40}$ to intraparenchymal amyloid in AD may be best achieved by conjugation of Aβ$^{1-40}$ to a BBB drug delivery system.

In summary, these studies show that conjugation of Aβ$^{1-40}$ to the SA-OX26 vector has the dual effects of reducing Aβ$^{1-40}$ metabolism and facilitating BBB transport of the peptide. Conjugation of Aβ$^{1-40}$ to the SA-OX26 delivery system does not impair saturable binding of the peptide to preexisting amyloid plaques in AD brain. Therefore, this delivery system has the potential for neuroimaging the Aβ amyloid in patients with AD by using external detection technology such as SPECT. This potential may be tested in animals that develop Aβ amyloid plaques in brain with aging. Aged rhesus or squirrel monkeys develop cerebral amyloid (25–27). However, the OX26 antibody vector is specific for rats (28), and to image brain amyloid, a BBB delivery vector must be available for the species under investigation. Recent studies show that the 83-14 mAb to the human insulin receptor is an active brain drug delivery vector in rhesus monkeys, but not squirrel monkeys (11). The 83-14 antibody is an active BBB transport vector, and the BBB PS product for the 83-14 mAb in the rhesus monkey

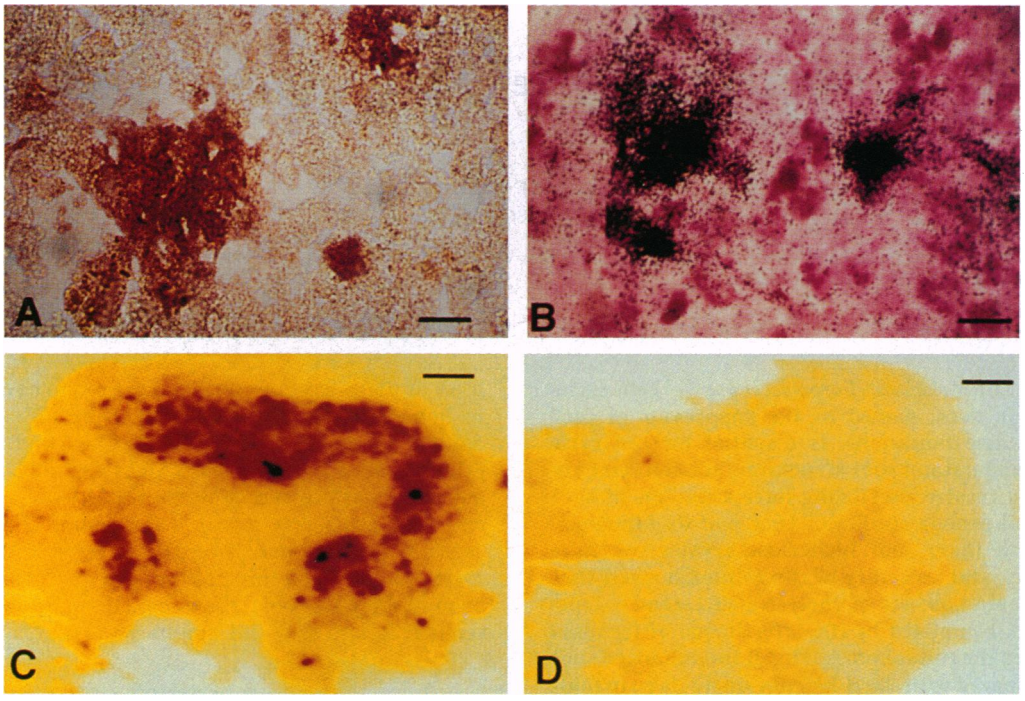

FIG. 5. (*A*) Immunocytochemistry with an anti-Aβ^{1-28} rabbit polyclonal antiserum and Formalin-fixed, formic acid-treated, frozen sections of AD brain. Neuritic plaques are immunostained with the anti-Aβ^{1-28} antiserum. (*B*) Emulsion autoradiography showing binding of ^{125}I,bio-Aβ^{1-40}/SA-OX26 conjugate to amyloid plaques of frozen sections of AD brain. The addition of 10 μM unlabeled Aβ^{1-40} completely inhibited binding of the conjugate to the amyloid plaques. (*C* and *D*) Film autoradiography showing binding of ^{125}I,bio-Aβ^{1-40}/SA-OX26 to plaques in frozen sections of AD brain in the presence of either 0 (*C*) or 10 μM (*D*) unlabeled Aβ^{1-40}. The studies show binding of the conjugate (Fig. 1) to amyloid in gray matter with minimal binding to the central white matter track. The binding to gray matter amyloid is abolished by the inclusion of 10 μM unlabeled Aβ^{1-40}. (Bars in *A* and *B* are 29 μm and those in *C* and *D* are 9 mm.)

is 8-fold greater than the BBB PS product for the OX26 mAb in the rat (11). The ability to semiquantitate and image amyloid in patients suspected of AD would not only provide a specific diagnostic test for this condition but also would provide a means of monitoring the effects of drug therapies aimed at reducing the Aβ amyloid burden in AD brain.

Emily Yu skillfully prepared the manuscript. The authors are indebted to Dr. Harry Vinters for providing the frozen AD autopsy brain. Y.S. is on leave from Snow Brand Milk Products Co., Ltd. (Tochigi, Japan). This work was supported by a grant from the American Health Assistance Foundation.

1. Dewan, M. J. & Gupta, S. (1992) *Comp. Psychol.* **33,** 282–290.
2. Tomlinson, B. E., Blessed, G. & Roth, M. (1970) *J. Neurol. Sci.* **22,** 205–242.
3. Glenner, G. G. & Wong, C. W. (1984) *Biochem. Biophys. Res. Commun.* **120,** 885–890.
4. Kang, J., Lemaire, H.-G., Unterbeck, A., Salbaum, J. M., Masters, C. L., Grzeschik, K.-H., Multhaup, G., Beyreuther, K. & Muller-Hill, B. (1987) *Nature (London)* **325,** 733–736.
5. Maggio, J. E., Stimson, E. R., Ghilardi, J. R., Allen, C. J., Dahl, C. E., Whitcomb, D. C., Vigna, S. R., Vinters, H. V., Labenski, M. E. & Mantyh, P. W. (1992) *Proc. Natl. Acad. Sci. USA* **89,** 5462–5466.
6. Pardridge, W. M. (1991) *Peptide Drug Delivery to the Brain* (Raven, New York).
7. Pardridge, W. M., Boado, R. J. & Kang, Y.-S. (1995) *Proc. Natl. Acad. Sci. USA* **92,** 5592–5596.
8. Bickel, U., Kang, Y.-S. & Pardridge, W. M. (1995) *Bioconjugate Chem.* **6,** 211–218.
9. Kang, Y.-S. & Pardridge, W. M. (1994) *J. Pharmacol. Exp. Ther.* **269,** 344–350.
10. Mattson, G., Conklin, E., Desai, S., Nielander, G., Savage, M. D. & Morgensen, S. (1993) *Mol. Biol. Rep.* **17,** 167–183.
11. Pardridge, W. M., Kang, Y.-S., Buciak, J. L. & Yang, J. (1995) *Pharm. Res.* **12,** 807–816.
12. Gibaldi, M. & Perrier, D. (1982) *Pharmacokinetics* (Dekker, New York).
13. Triguero, D., Buciak, J. B. & Pardridge, W. M. (1990) *J. Neurochem.* **54,** 1882–1888.
14. Vinters, H. V., Pardridge, W. M., Secor, D. L. & Ishii, N. (1988) *Am. J. Pathol.* **133,** 150–162.
15. Samii, A., Bickel, U., Stroth, U. & Pardridge, W. M. (1994) *Am. J. Physiol.* **267,** E124–E131.
16. Oldendorf, W. H., Hyman, S., Braun, L. & Oldendorf, S. Z. (1972) *Science* **178,** 984–986.
17. Zlokovic, B. V., Ghiso, J., Mackic, J. B., McComb, J. G., Weiss, M. H. & Frangione, B. (1993) *Biochem. Biophys. Res. Commun.* **197,** 1034–1040.
18. Glabe, C., Burdick, D. & Yang, A. (1995) *J. Cell. Biochem.*, Suppl. 21B, 103.
19. Watson, D. J. & Selkoe, D. J. (1994) *Soc. Neurosci. Abstr.* **20,** 1642.
20. Nordstedt, C., Näslund, J., Tjernberg, L. O., Karlström, A. R., Thyberg, J. & Terenius, L. (1994) *J. Biol. Chem.* **269,** 30773–30776.
21. Pardridge, W. M., Vinters, H. V., Yang, J., Eisenberg, J., Choi, T., Tourtellotte, W. W., Huebner, V. & Shively, J. E. (1987) *J. Neurochem.* **49,** 1394–1401.
22. Roher, A. E., Lowenson, J. D., Clarke, S., Woods, A. S., Cotter, R. J., Gowing, E. & Ball, M. J. (1993) *Proc. Natl. Acad. Sci. USA* **90,** 10836–10840.
23. Zhang, E. T., Inman, C. B. E. & Weller, R. O. (1990) *J. Anat.* **170,** 111–123.
24. Schlageter, N. L., Carson, R. E. & Rapoport, S. I. (1987) *J. Cereb. Blood Flow Metab.* **7,** 1–8.
25. Walker, L. C., Masters, C., Beyreuther, K. & Price, D. L. (1990) *Acta Neuropathol.* **80,** 381–387.
26. Martin, L. J., Sisodia, S. S., Koo, E. H., Cork, L. C., Dellovade, T. L., Weidemann, A., Beyreuther, K., Masters, C. & Price, D. L. (1991) *Proc. Natl. Acad. Sci. USA* **88,** 1461–1465.
27. Walker, L. C., Price, D. L., Voytko, M. L. & Schenk, D. B. (1994) *J. Neuropathol. Exp. Neurol.* **53,** 377–383.
28. Jefferies, A. W., Brandon, M. R., Williams, A. F. & Hunt, S. V. (1985) *Immunology* **54,** 333–341.